



**AALBORG UNIVERSITY**  
DENMARK

**Aalborg Universitet**

## **Bi-Level Programming for Integrating Flexible Demand in Combined Smart Energy System**

Xi, Yufei; Hamacher, Thomas; Peri, V.; Vedran; Chen, Zhe; Lund, Henrik

*Published in:*  
7th IEEE International Smart Cities Conference (ISC2 2021)

*DOI (link to publication from Publisher):*  
[10.1109/ISC253183.2021.9562967](https://doi.org/10.1109/ISC253183.2021.9562967)

*Publication date:*  
2021

*Document Version*  
Accepted author manuscript, peer reviewed version

[Link to publication from Aalborg University](#)

*Citation for published version (APA):*  
Xi, Y., Hamacher, T., Peri, V., Chen, Z., & Lund, H. (2021). Bi-Level Programming for Integrating Flexible Demand in Combined Smart Energy System. In *7th IEEE International Smart Cities Conference (ISC2 2021)* (pp. 1-6) <https://doi.org/10.1109/ISC253183.2021.9562967>

### **General rights**

Copyright and moral rights for the publications made accessible in the public portal are retained by the authors and/or other copyright owners and it is a condition of accessing publications that users recognise and abide by the legal requirements associated with these rights.

- Users may download and print one copy of any publication from the public portal for the purpose of private study or research.
- You may not further distribute the material or use it for any profit-making activity or commercial gain
- You may freely distribute the URL identifying the publication in the public portal -

### **Take down policy**

If you believe that this document breaches copyright please contact us at [vbn@aub.aau.dk](mailto:vbn@aub.aau.dk) providing details, and we will remove access to the work immediately and investigate your claim.

# Bi-Level Programming for Integrating Flexible Demand in Combined Smart Energy System

Yufei Xi  
Dept. of Energy Technology  
Aalborg University  
Aalborg, Denmark  
yux@et.aau.dk

Thomas Hamacher  
Renewable and Sustainable Energy  
Systems  
Technical University of Munich  
Munich, Germany  
thomas.hamacher@tum.de

Vedran Perić  
Renewable and Sustainable Energy  
Systems  
Technical University of Munich  
Munich, Germany  
vedran.peric@tum.de

Zhe Chen  
Dept. of Energy Technology  
Aalborg University  
Aalborg, Denmark  
zch@et.aau.dk

Henrik Lund  
Dept. of Planning  
Aalborg University  
Aalborg, Denmark  
lund@plan.aau.dk

**Abstract**—In this paper, a gas-electricity-heat integrated energy system with smart buildings is described. The special focus is flexible energy demand including electricity and heat integrated into the smart buildings, where customers have multiple options to satisfy their energy demand. Considering energy prices in the market, the aggregator is introduced to manage these smart buildings in the most economical way. This paper proposes a bi-level programming approach for the integration of flexible demand in the combined smart energy system (CoSES). The integrated system operator (ISO) aims at maximizing social welfare according to the operation strategy of the aggregator, which minimizes the energy purchase cost of downstream demand. Then, the linearization method and Karush-Kuhn-Tucker (KKT) conditions are used to transform the bi-level optimization problem into an easily handled single-level problem. The proposed approach is illustrated in a modified test system.

**Keywords**—integrated energy system, smart building, flexibility, bi-level optimization, dispatch model, district heating

## NOMENCLATURE

### Sets and indices

$T$	Set of time horizon
$N_b$	Set of buildings integrated to aggregator
$N_{\text{EPS/NGS/DHS}}$	Set of nodes of electric power system/ natural gas system/district heating system
$N_\Phi$	Set of energy units $\Phi$
$N_{gl}$	Set of load nodes in gas system
<b>Parameter</b>	
$s$	
$B^{e/g/h}$	Benefit coefficient of power/gas/heat demand
$c_i^\Phi$	Cost coefficient of energy unit $\Phi$ at node $i$
$I_{i,t}^{e/g/h}$	Hourly electricity/gas/heat load at node $i$
$T_i^{s,in}$	Inlet temperature of supply pipe $i$
$T_t^a$	Ambient temperature at time $t$
$P_{i,t}^W, P_{i,t}^{PV}$	Output of wind and photovoltaic at node $i$
$G_{ij}, B_{ij}$	Conductance and susceptance of power line $i$ - $j$
$Z_{ij}$	Resistance coefficient of gas pipe $i$ - $j$
$COP_i$	Coefficient of performance of heat pump $i$

$\eta_i^\Phi$	Conversion factor of energy unit $\Phi$ at node $i$
$\sigma$	Heat loss coefficient of heat storage
$r_i^{\text{CHP}}$	Heat to power ratio of CHP unit $i$
$x_i$	Pipe length
$v$	Water velocity
$\omega$	Angular frequency
$k / k^{\text{wp}}$	Convective heat transfer coefficient between environment and pipe outer wall/flow and pipe inner wall
$L^{\text{in/ex}}$	Internal/exterior perimeter of pipe wall
$c / c^{\text{p}}$	Specific heat of water and pipe wall
$A / A^{\text{p}}$	Cross-sectional area of water flow /pipe wall
$\rho / \rho^{\text{p}}$	Density of water/pipe wall
<b>Variables</b>	
$D_{i,t}^{\text{eh}}$	Hourly power/heat demand of building $i$ (MW)
$P_{i,t}^{\text{CHP}}$	Hourly power output of CHP unit $i$ (MW)
$P_{i,t}^{\text{CFP}}$	Hourly power output of CFP unit $i$ (MW)
$P_{i,t}^{\text{W-gc}}$	Hourly power output from wind unit $i$ (MW)
$P_{i,t}^{\text{PV-gc}}$	Hourly power output from PV unit $i$ (MW)
$P_{i,t}^{\text{P2G}}$	Hourly power consumption of P2G $i$ (MW)
$P_{i,t}^{\text{HP}}$	Hourly power consumption of HP $i$ (MW)
$P_{i,t}^{\text{EV}_{in/out}}$	Hourly input/output of EV storage at node $i$ (MW)
$G_{i,t}^{\text{SN}}$	Hourly gas generation of gas source $i$ (MW)
$G_{i,t}^{\text{GS}_{in/out}}$	Hourly gas input/output of gas storage $i$ (MW)
$G_{i,t}^{\text{P2G}}$	Hourly gas output of P2G unit $i$ (MW)
$G_{i,t}^{\text{CHP}}$	Hourly gas consumption of CHP unit $i$ (MW)
$G_{i,t}^{\text{GB}}$	Hourly gas consumption of GBs $i$ (MW)
$H_{i,t}^{\text{CHP}}$	Hourly heat output of CHP unit $i$ (MW)
$H_{i,t}^{\text{HS}_{in/out}}$	Hourly heat input/output of heat storage $i$ (MW)
$H_{i,t}^{\text{HP}}$	Hourly heat output of HP $i$ (MW)
$H_{i,t}^{\text{GB}}$	Hourly heat output of GBs $i$ (MW)
$SOC_{i,t}^{\text{GS}}$	Hourly stock state of gas storage $i$ (MWh)

$SOC_{i,t}^{EV}$	Hourly stock state of EV storage $i$ (MWh)
$SOC_{i,t}^{HS}$	Hourly stock state of heat storage $i$ (MWh)
$\theta_{i,t}, V_{i,t}$	Hourly phase angle and voltage of bus $i$ (rad)
$P_{i,t}$	Hourly nodal gas pressure (MPa)
$H_{i,t}^{loss}$	Hourly heat loss of heat pipe $i$ (MW)
$T_{i,t}^{s,out}$	Hourly outlet temperature of supply pipe $i$ (°C)
$T_{i,t}^{r,in/out}$	Hourly inlet/outlet temperature of return pipe $i$ (°C)
$p_i^e / p_i^g$	Hourly electricity/gas price

## I. INTRODUCTION

The integration of multiple energy systems (gas, electricity, heating or cooling and transportation) has been recognized as an effective measure to change to renewable energy systems [1]. However, the variability and uncertainty of renewable energy bring new challenges to the operation of modern power systems. More flexible measures are urgently needed to ensure the balance between supply and demand over time.

The traditional system flexibility is almost achieved by controlling generation units and coordinating transmission and distribution [2]. However, energy integration allows multiple options to meet customers' energy demands. In return, customers with controllable demand, distributed generation and storage can adjust power flows in synergy with the upper network's needs to provide additional flexibility on the demand side [3], [4]. For example, the CoSES Laboratory in TU Munich emulates a small microgrid, in which the consumers are simulated as buildings with photovoltaic power (PV) generation, electric vehicle (EV) chargers and electric heaters [5]. The heat demand for these smart buildings can be supplied by heat networks and electric heating devices, such as electric boilers or heat pumps (HPs). Such built-in flexibility of consumers is of great significance to the operating efficiency and economy of integrated energy systems. In [6], a multi-objective optimization model of a synergetic dispatch for building management is proposed. In [7], a bi-level optimization problem of the electricity-heat integrated system is proposed, where customer aggregators are introduced to supply downstream demand in the most economical way. In [8], the PV-generated electricity from households is integrated into the energy system and a bidding strategy in the local electricity market is proposed. In [9], a bi-level programming approach for the collaborative management of active distribution networks by designing comprehensive prices is proposed. These studies adjust the consumers' demand by using the bid information in markets and optimize the operation of the integrated energy system. However, these works focus on integrating electricity and heat on the level of energy distribution, whereas gas systems and gas markets are rarely considered.

Actually, the natural gas system (NGS) and the district heating system (DHS) are closely related. Gas-fired combined heat and power (CHP) units and gas-fired boilers (GBs) play important roles in heat supply. This paper describes a CoSES with smart buildings in which the gas system and market are both considered. The aggregator controlling the smart buildings is introduced into the centralized dispatch model on the transmission level. Therefore, a bi-level optimization

problem is formulated, where the upper-objective maximizes social welfare subject to the optimal operation of the aggregator, which minimizes the energy purchase cost of downstream demand.

The remainder of the paper is organized as follows. Section II presents the structure of the CoSES with smart buildings and describes the formulation of the bi-level optimization dispatch model and its solution methodology. Section III presents and analyzes the corresponding simulation results in the test system. Section IV gives the conclusion of the research work.

## II. MODEL FORMULATION

### A. Description of the CoSES

The proposed CoSES is an integration of gas, electricity and heat systems based on smart buildings. Fig.1 shows the schematic graph of the proposed CoSES. The system consists of energy generation units, conversion units, storage units, energy networks, and customers' energy demand.

As far as the entire CoSES is concerned, energy generation units include conventional generators such as coal-fired power plants (CFP), renewable energy generators such as solar units and wind power (WP) units, and gas source nodes. The conversion units include combined heat and power (CHP) units, gas boilers (GBs), and P2G units. The heat generated by the CHP unit and GB is transported to the demand side through the district heating (DH) network and distributed to the building through the heat station. When the wind power is surplus or the electricity price is low, P2G units consume electricity to supply gas. In addition, the heat and gas storage are installed in the CoSES to provide the necessary flexibility.

Electricity and heat demands are composed of smart building clusters. Fig. 2 shows the schematic diagram of a smart building. These buildings can be treated as a composite load by connecting solar panels, electric vehicle (EV) chargers with energy storage, electric heaters, and multiple power outlets (driving household appliances) in parallel. Each smart building represents an integrated electricity and heat prosumer, which is connected to the power distribution network and the DH network.

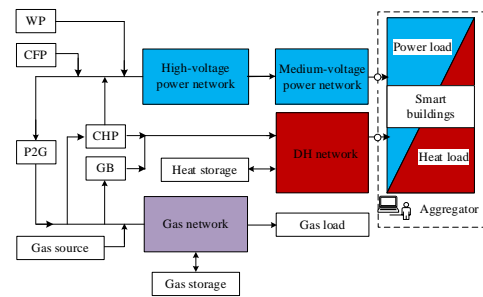


Fig. 1. The schematic graph of the CoSES

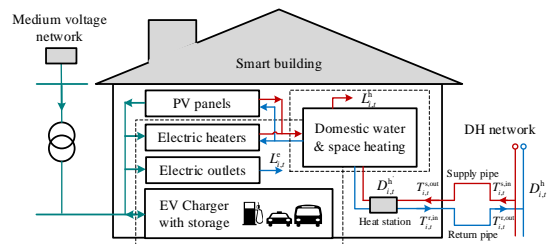


Fig. 2. The schematic diagram of a smart building

These smart buildings are integrated, operated and controlled by the aggregator in which the sub-aggregator groups a number of buildings into a cluster for the purpose of carrying more weight on the demand side. The aggregator acts as a mediator between the utility and customers. On the one hand, the aggregator represents smart buildings to participate in the market and provide flexible demand to the upper grid. On the other hand, guaranteeing a minimization in the energy bills of customers, the aggregator satisfies electricity and heat demands in buildings by coordinating the internal operation of PV, electric heating, EV charging and electricity storage. Thus, the aggregator can be modeled as an integrated electricity and heat demand node.

### B. Bi-level Optimization of Dispatch Model

In this section, there are two assumptions as follows: 1) An integrated system operator (ISO), in charge of managing gas, electricity and heat subsystems, runs a centralized dispatch model for scheduling the CoSES; 2) The aggregator has its own service platform for data analysis that can interact with the complex adaptive system of the upper power system and provide valuable information for the lower smart buildings including weather conditions, market decisions and operating arrangements. From Fig. 1, the DH network with heat load can be considered as a pure consumer in the market. The real-time price mechanisms in the gas and electricity markets can provide economic incentives. The aggregator that integrates smart buildings can use these incentives to minimize energy purchase costs by adjusting the energy consumption patterns of these buildings. In return, the aggregator's response provides additional flexibility to the entire CoSES as well as uncertainty for the CoSES operation.

Generally, it can be assumed that the aggregator is a market participant who strives to decrease energy purchase costs. In consequence, a bi-level optimization problem is formulated for describing the centralized dispatch model of the CoSES. In the upper-level problem, the ISO aims at maximizing social welfare according to bid results in the market. In the lower-level problem, the aggregator minimizes the energy purchase cost based on the real-time energy prices. More specifically, after receiving the clearing quantity and price issued by the market operator, the aggregator proposes the solution for minimizing purchase energy costs and sends information to the ISO. Afterwards, the ISO obtains the optimal strategy for the total CoSES by running the centralized energy dispatch model.

The bi-level optimization is formulated as shown in (1)–(32).

$$\begin{aligned} \text{Maximize}_{G_{i,t}^{\text{CHP}}, G_{i,t}^{\text{SN}}, P_{i,t}^{\text{GS\_in}}, P_{i,t}^{\text{HS\_in}}} F = & \sum_{t=1}^T \left( \sum_{i=1}^{N_b} (B^e D_{i,t}^e + B^h D_{i,t}^h) + \sum_{i=1}^{N_{gl}} B^g L_{i,t}^g \right. \\ & \left. - \left( \sum_{i=1}^{N_c} c_i^{\text{CFP}} P_{i,t}^{\text{CFP}} + \sum_{i=1}^{N_m} c_i^{\text{SN}} G_{i,t}^{\text{SN}} \right) \right. \\ & \left. - \left( \sum_{i=1}^{N_{gs}} c_i^{\text{GS}} G_{i,t}^{\text{GS\_in}} + \sum_{i=1}^{N_{hs}} c_i^{\text{HS}} H_{i,t}^{\text{HS\_in}} \right) \right) \end{aligned} \quad (1)$$

Subject to:

$$\begin{aligned} & \sum_{i \in N_c} P_{i,t}^{\text{CFP}} + \sum_{i \in N_g} P_{i,t}^{\text{CHP}} + \sum_{i \in N_w} P_{i,t}^{\text{W\_gc}} - \sum_{i \in N_p} P_{i,t}^{\text{P2G}} - \sum_{i \in N_b} D_{i,t}^e \\ & = \sum_{i,j \in N_{\text{EPS}}} V_i V_j \left[ G_{ij} \cos(\theta_{i,t} - \theta_{j,t}) + B_{ij} \sin(\theta_{i,t} - \theta_{j,t}) \right] \end{aligned} \quad (2)$$

$$\begin{aligned} & \sum_{i \in N_g} H_{i,t}^{\text{CHP}} + \sum_{i \in N_{gb}} H_{i,t}^{\text{GB}} \\ & + \sum_{i \in N_{hs}} (H_{i,t}^{\text{HS\_out}} - H_{i,t}^{\text{HS\_in}}) = \sum_{i \in N_b} D_{i,t}^h \end{aligned} \quad (3)$$

$$\begin{aligned} & \sum_{i \in N_{sn}} G_{i,t}^{\text{SN}} + \sum_{i \in N_p} G_{i,t}^{\text{P2G}} + \sum_{i \in N_{gs}} (G_{i,t}^{\text{GS\_out}} - G_{i,t}^{\text{GS\_in}}) \\ & - \sum_{i \in N_g} G_{i,t}^{\text{CHP}} - \sum_{i \in N_{gb}} G_{i,t}^{\text{GB}} - \sum_{i \in N_{gl}} L_{i,t}^g = \sum_{i,j \in N_{\text{DHS}}} \sqrt{\frac{P_{i,t}^2 - P_{j,t}^2}{Z_{ij}}} \end{aligned} \quad (4)$$

$$\overline{P_{i,t}^{\text{CFP}}} \leq P_{i,t}^{\text{CFP}} \leq \overline{P_{i,t}^{\text{CFP}}}, \forall i \in N_c \quad (5)$$

$$\overline{P_{i,t}^{\text{CHP}}} \leq P_{i,t}^{\text{CHP}} \leq \overline{P_{i,t}^{\text{CHP}}}, \forall i \in N_g \quad (6)$$

$$0 \leq P_{i,t}^{\text{W\_gc}} \leq P_{i,t}^{\text{W}}, \forall i \in N_w \quad (7)$$

$$\overline{P_{i,t}^{\text{P2G}}} \leq P_{i,t}^{\text{P2G}} \leq \overline{P_{i,t}^{\text{P2G}}}, \forall i \in N_p \quad (8)$$

$$\overline{H_{i,t}^{\text{GB}}} \leq H_{i,t}^{\text{GB}} \leq \overline{H_{i,t}^{\text{GB}}}, \forall i \in N_{gb} \quad (9)$$

$$\overline{G_{i,t}^{\text{SN}}} \leq G_{i,t}^{\text{SN}} \leq \overline{G_{i,t}^{\text{SN}}}, \forall i \in N_{sn} \quad (10)$$

$$-\overline{P_{ij,t}}, \leq P_{ij,t} \leq \overline{P_{ij,t}}, \forall ij \in N_{\text{EPS}} \quad (11)$$

$$-\overline{G_{ij,t}}, \leq G_{ij,t} \leq \overline{G_{ij,t}}, \forall ij \in N_{\text{NGS}} \quad (12)$$

$$P_{i,t}^{\text{CHP}} = r_i^{\text{CHP}} \cdot H_{i,t}^{\text{CHP}}, \forall i \in N_g \quad (13)$$

$$P_{i,t}^{\text{CHP}} = \eta_i^{\text{CHP}} G_{i,t}^{\text{CHP}}, \forall i \in N_g \quad (14)$$

$$G_{i,t}^{\text{P2G}} = \eta_i^{\text{P2G}} P_{i,t}^{\text{P2G}}, \forall i \in N_p \quad (15)$$

$$H_{i,t}^{\text{GB}} = \eta_i^{\text{GB}} \cdot G_{i,t}^{\text{GB}}, \forall i \in N_{gb} \quad (16)$$

$$\begin{cases} \overline{G_{i,t}^{\text{GS\_in/out}}} \leq G_{i,t}^{\text{GS\_in/out}} \leq \overline{G_{i,t}^{\text{GS\_in/out}}} \\ \text{SOC}_{i,t}^{\text{GS}} - \text{SOC}_{i,t-1}^{\text{GS}} = (G_{i,t}^{\text{GS\_in}} - G_{i,t}^{\text{GS\_out}}) \Delta t \\ \overline{\text{SOC}_{i,t}^{\text{GS}}} \leq \text{SOC}_{i,t}^{\text{GS}} \leq \overline{\text{SOC}_{i,t}^{\text{GS}}} \\ \text{SOC}_{i,t_0}^{\text{GS}} = \text{SOC}_{i,t_N}^{\text{GS}} \quad \forall i \in N_{gs}, \forall t \in T \end{cases} \quad (17)$$

$$\begin{cases} \overline{H_{i,t}^{\text{HS\_in/out}}} \leq H_{i,t}^{\text{HS\_in/out}} \leq \overline{H_{i,t}^{\text{HS\_in/out}}} \\ \text{SOC}_{i,t}^{\text{HS}} - \sigma \text{SOC}_{i,t-1}^{\text{HS}} = \left( H_{i,t}^{\text{HS\_in}} \eta_i^{\text{HS\_in}} - \frac{H_{i,t}^{\text{HS\_out}}}{\eta_i^{\text{HS\_out}}} \right) \Delta t \\ \overline{\text{SOC}_{i,t}^{\text{HS}}} \leq \text{SOC}_{i,t}^{\text{HS}} \leq \overline{\text{SOC}_{i,t}^{\text{HS}}} \\ \text{SOC}_{i,t_0}^{\text{HS}} = \text{SOC}_{i,t_N}^{\text{HS}} \quad \forall i \in N_{hs}, \forall t \in T \end{cases} \quad (18)$$

$$\begin{aligned} (D_{i,t}^e, D_{i,t}^h) \in \arg \text{ minimize } f = & \begin{bmatrix} P_t^e \\ P_t^g \end{bmatrix} \cdot \sum_{i \in N_b} (D_{i,t}^e + D_{i,t}^h) \\ & = p_t^g (G_{i,t}^{\text{CHP}} + G_{i,t}^{\text{GB}}) - p_t^e P_{i,t}^{\text{P2G}} \end{aligned} \quad (19)$$

$$\sum_{i \in N_b} (D_{i,t}^e) = \sum_{i \in N_b} (L_{i,t}^e + P_{i,t}^{\text{HP}} + (P_{i,t}^{\text{EV\_in}} - P_{i,t}^{\text{EV\_out}}) - P_{i,t}^{\text{PV\_gc}}) \quad (20)$$

$$\sum_{i \in N_b} (D_{i,t}^h - H_{i,t}^{\text{loss}}) = \sum_{i \in N_b} (D_{i,t}^h) = \sum_{i \in N_b} (L_{i,t}^h - H_{i,t}^{\text{HP}}) \quad (21)$$

$$D_{i,t}^h = cm_i (T_{i,t}^{\text{s,in}} - T_{i,t}^{\text{r,out}}), \forall i \in N_s \quad (22)$$

$$D_{i,t}^h = c \cdot m_i \cdot (T_{i,t}^{\text{s,out}} - T_{i,t}^{\text{r,in}}), \forall i \in N_s \quad (23)$$

$$\begin{cases} T_{i,t}^{s,out} = \varphi_i \cdot T_{i,t-\alpha_i}^{s,in} + T_i^a \cdot (1 - \varphi_i) \\ T_{i,t}^{r,out} = \varphi_i \cdot T_{i,t-\alpha_i}^{r,in} + T_i^a \cdot (1 - \varphi_i) \end{cases} \quad (24)$$

$$\alpha_i = \frac{x_i}{v} \cdot \left( 1 + \frac{h_1 h_2}{\left( \omega^2 + (h_1 + h_2)^2 \right)} \right) \quad (25)$$

$$\varphi_i = \exp \left( - \frac{h x_i}{v} \cdot \left( 1 - \frac{h_1 (h_1 + h_2)}{\left( \omega^2 + (h_1 + h_2)^2 \right)} \right) \right) \quad (26)$$

$$h = \frac{k^{wp} L^{in}}{Ac \rho}, \quad h_1 = \frac{k^{wp} L^{in}}{A^p c^p \rho^p}, \quad h_2 = \frac{k L^{ex}}{A^p c^p \rho^p} \quad (27)$$

$$0 \leq P_{i,t}^{PV-gc} \leq P_{i,t}^{PV}, \quad \forall i \in N_w \quad (28)$$

$$P_{i,t}^{HP} \leq P_{i,t}^{HP} \leq \overline{P_{i,t}^{HP}}, \quad \forall i \in N_{hp} \quad (29)$$

$$H_{i,t}^{PV} = \eta_i^{PV} \cdot P_{i,t}^{PV}, \quad \forall i \in N_{pv} \quad (30)$$

$$H_{i,t}^{HP} = COP_i \cdot P_{i,t}^{HP}, \quad \forall i \in N_{hp} \quad (31)$$

$$\begin{cases} \underline{P_{i,t}^{EV,in/out}} \leq P_{i,t}^{EV,in/out} \leq \overline{P_{i,t}^{EV,in/out}} \\ SOC_{i,t}^{EV} - SOC_{i,t-1}^{EV} = (G_{i,t}^{EV,in} - G_{i,t}^{EV,out}) \Delta t \\ \underline{SOC_{i,t}^{EV}} \leq SOC_{i,t}^{EV} \leq \overline{SOC_{i,t}^{EV}} \\ SOC_{i,t_0}^{EV} = SOC_{i,t_N}^{EV} \quad \forall i \in N_{ev}, \forall t \in T \end{cases} \quad (32)$$

The upper-level problem shown in (1)–(18) represents the centralized scheduling of the CoSES with the objective of maximizing social welfare. Equation (1) has four components, including the benefit of energy demand controlled by the aggregator, the benefit of gas load, the fuel costs of CFPs, the gas sources node, and the operation costs of gas and heat storage. Equations (2), (3) and (4) represent the nodal power balance, heat balance and nodal gas balance, respectively. Since the upper-level problem focuses on the transmission network, the DH network connected to the aggregator can be equivalent to a heat demand node, in which only the heat balance is taken into account in equation (3). Equations (5)–(10) represent energy output bounds for the CFP unit, the CHP unit, the wind farm, the P2G unit, the gas boiler and the gas source node, respectively. Constraints (11) and (12) enforce the transmission capacity limits of each electricity line and gas pipe. Constraints (13)–(16) represent the heat-to-electricity ratio of the CHP unit, the energy conversion ratio of the CHP unit, the P2G unit and the GB unit, respectively. Equations (17) and (18) express the operational constraints of gas storage and heat storage, respectively. Each equation has four components, including the constraints of charging/discharging power, the hourly state of charge (SOC), the bounds for SOC and the recovery of energy storage.  $t_0$  and  $t_N$  are the initial and final time of the time horizon  $T$ . The electricity demand and heat demand ( $\sum_{i \in N_b} D_{i,t}^e$ ,  $\sum_{i \in N_b} D_{i,t}^h$ ) from the aggregator are generated in the lower-level problem.

The lower-level problem (19)–(32) represents the operation strategy of the aggregator that aims at minimizing the energy purchase cost.  $p_t^e$  and  $p_t^g$  are the real-time electricity price and the gas price in the market. Equations (20) and (21) represent power balance and heat balance of the aggregator, respectively. Since the lower-level problem focuses on the heat transfer in the DH network, the assumptions are proposed as follows: 1) Each secondary DH

network is simplified to a heat station that directly supplies heat to the smart building; 2) The DHS adopts the heating method for constant flow and variable temperature (CFVT). As shown in Fig.2, the heat produced from the heat sources is transferred to the heat station through the DH network. Equations (22) and (23) define the relationship between nodal heat power, water mass flow, and the inlet/outlet temperature of the supply pipe and the return pipe. The dynamic variation of the water temperature in the DH network is reflected in time and space. Thus, two important parameters of lag time  $\alpha_i$  and relative attenuation degree  $\varphi_i$  are introduced in reference [10] to describe the temperature change along the pipe in equations (27).  $\alpha_i$  and  $\varphi_i$  are defined by equations (25) and (26), while the corresponding parameters are given in equation (27). Equations (28) and (29) represent the bounds of energy power output for the PV unit and the HP unit, respectively. Equations (30) and (31) represent the electricity-to-heat ratio of the PV unit and the HP unit, respectively. Due to the installed PV unit, the EV charger with storage is considered in each smart building. These chargers enable the buildings to charge/discharge the EVs, as well as storage the surplus electricity. For example, the buildings can use the electricity stored after PV power generation during the day to charge EVs even at night. Equation (32) defines the operational constraints of the EV charger with storage.

Since equation (4) is non-convex in the upper-level problem, it needs to be linearized through the approach proposed in [11]. On the other hand, the common method to solve a bi-level optimization problem is to rewrite it as a standard optimization problem using KKT conditions [12]. In this paper, the IPOPT solver under the platform GAMS is used to solve the proposed optimization model. In summary, the aggregator sends the ISO a demand plan. According to the bid information, the ISO conducts a centralized dispatch. The flowchart of the optimization procedures is shown in Fig. 3.

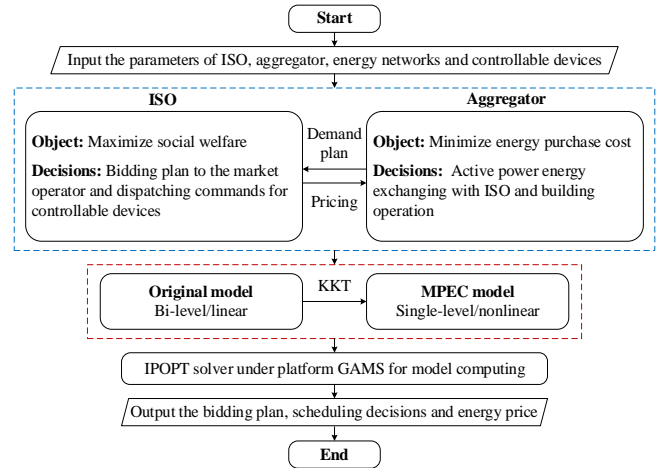


Fig. 3. Flowchart of the optimization procedures

### III. CASE STUDY

#### A. Description of the Test System

In this section, the integration of an IEEE RTS 24-bus EPS, a 4-node NGS and a 20-node DHS is proposed in Fig. 4. The DHS includes 20 nodes, 12 heat stations and 38 pipes. The heat sources include CHPs, GB, PV and HPs. Heat storage is installed at node 20. The heat stations can directly supply heat to local smart buildings. The NGS has one gas source node and one load node. Gas storage and the GB are installed in the gas system. Besides, the improved IEEE RTS

24-bus system is shown in Fig. 5. W1-W4 are wind farms. A 60 MW P2G is installed at Bus 18, corresponding to gas node 4 in the gas system. G1-G3 are CHPs, with capacities 200 MW, 200 MW and 400 MW respectively. C1-C3 are CFPs, with capacities 200 MW, 200 MW and 600 MW respectively.

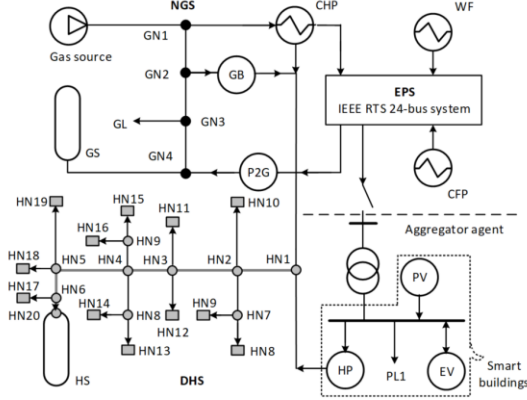


Fig. 4. Topology diagram of the CoSES

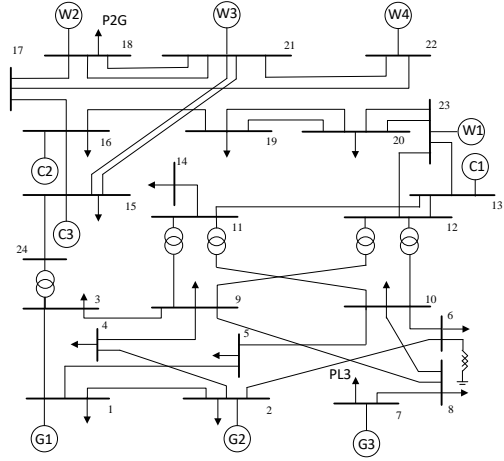


Fig. 5. The improved IEEE RTS 24-bus system

The historical data for Denmark on February 6, 2021 from Energinet.dk [13] is used and shown in Fig. 6, including wind power profile, electrical load, heat load, gas load, as well as PV power profile marked on the secondary axis.

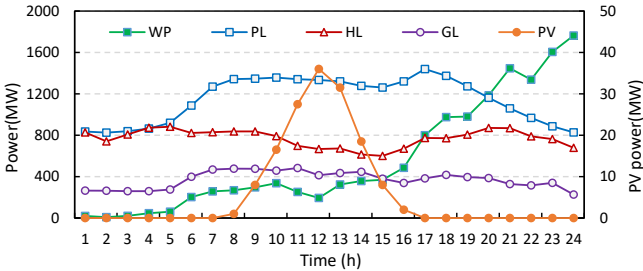


Fig. 6. Profiles of test data

### B. Simulation Results

In a 24-hour time horizon, Fig. 7 (a), (b) and (c) respectively show the optimal hourly output of electricity, heat and gas sources at the maximum social welfare of the CoSES. It should be noted that in order to avoid the expensive cost of start-up and shutdown, large generators such as CFPs and CHPs are limited to maintain their minimum outputs instead of a shutdown during the short-term scheduling.

In Fig. 6, periods 1-7h are under a low-wind condition. The wind power generation starts to increase from time 16h and reaches the peak at time 24h. During periods 1-7h, there is no heat produced by wind power. However, the peak-load periods of the DHS are the valley-load periods of the EPS. Each CHP forces electricity production when it supplies heat, which makes the surplus electricity available for HPs. During periods 8-15h, the electricity load increases, while the heat load gradually decreases to the valley. As the output of PV increases, the DHS prioritizes PV to supply heat. To balance heat production and consumption, the heat production of CHPs decreases. As a result, the electricity generation of CFPs increases. In Fig. 7 (d), the electricity price increases from 60.03 €/MWh to 80 €/MWh, which is equal to the marginal cost of CFPs. At time 9h, the gas load is the peak as well as the electricity load. The large demand for gas causes the gas price to rise from 67.23 €/MWh to a peak of 89.6 €/MWh. Periods 16-24h are under a high-wind condition. With the decrease in electrical load, the electricity price decreases. This promotes the NGS and DHS encourage P2G units and HPs to produce gas and heat respectively. Thus, the decrease in gas load and increase in gas generation from P2G units make a reduction of gas price. The surplus wind power is fully utilized. However, there is still wind power curtailment. The P2G or HP could not convert all the surplus wind power to gas or heat because of its capacity limitation.

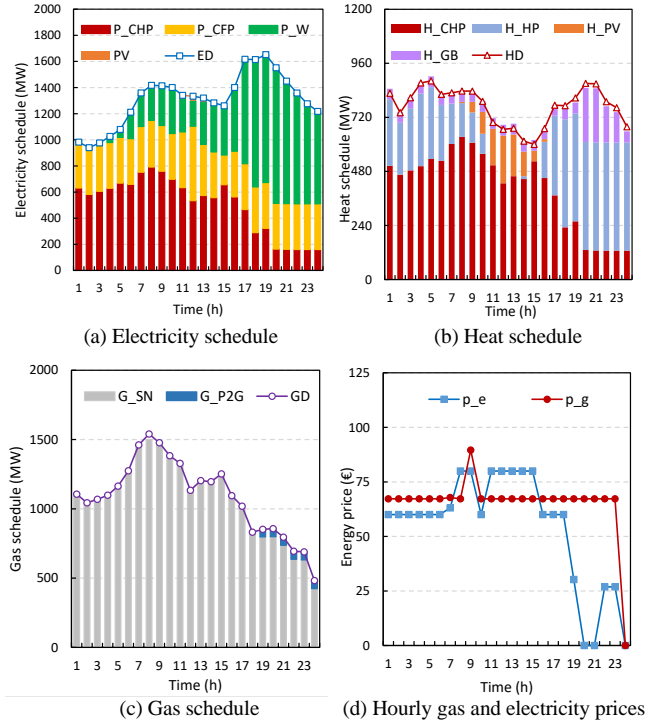


Fig. 7. Optimal schedule of sources in the CoSES

Fig. 8 (c) is the charge/discharge process of the EV chargers with storage. Especially for the EV chargers integrated with PV and storage, the surplus power can be used to charge EVs or stored in the batteries. During periods 1-3h, 8-13h, and 15-16h, the storage discharges to supply electricity. For the short periods 4-7h and 14h, it is better to use quick charging or battery replacement for EVs. For the long periods 17-24h, EVs can be charged slowly. It is consistent with the actual expectation in Section II.

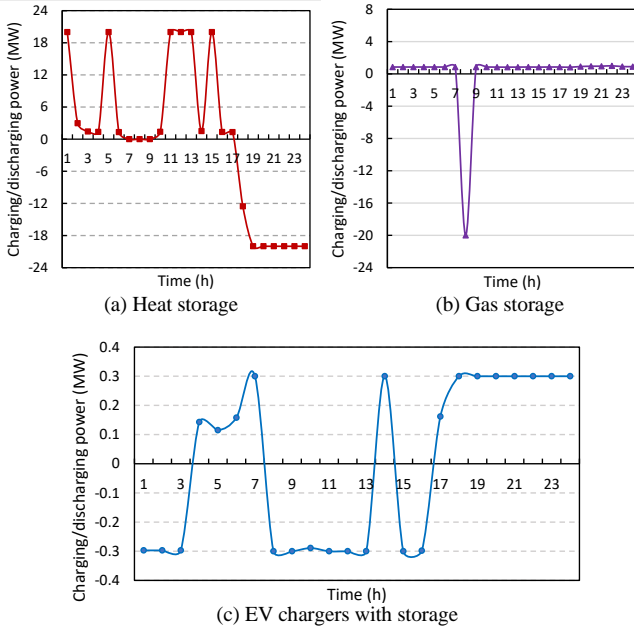


Fig. 8. Hourly charging/discharging power of storage units

To verify the advantages of integrating flexible demand in the CoSES, scenario 1 is introduced as a comparison. In scenario 1, there are no HPs and EV chargers installed in the buildings. The electricity and heat demands of the building interior are independently supplied through the external energy network. In other words, the buildings no longer have the ability to convert electricity to heat and support electricity charging and discharging because of the uninstallation of HPs and EV in scenario 1. Scenario 2 is the proposed CoSES with the buildings that have flexible demand. The simulation results are shown in Tab.1, including social welfare (SW) of the CoSES, energy purchase cost (EPC) of the aggregator, wind curtailment rate (WCR) and the used capacity (UC) of gas storage and heat storage.

See from Tab. 1, the total social welfare is higher and energy purchase cost is lower in scenario 2. The wind curtailment rates of scenario 1 and scenario 2 are 61.70% and 22.36%, respectively. The simulation result suggests that the smart buildings provide great flexibility and improve wind accommodation of the upper power network through such integration of HPs and EV chargers with storage. Moreover, compared with scenario 1, the used capacity of energy storage decreases in scenario 2, which may lead to the reduced investment of storage capacity for the CoSES.

TABLE I. COMPARISONS WITH TWO SCENARIOS

Unit	Scenario 1	Scenario 2
SW	879,410 €	1,434,500 €
EPC	2,061,253 €	1,146,819 €
WCR	61.70%	22.36%
UC <sub>GS</sub>	23.92MWh	14.10MWh
UC <sub>HS</sub>	150.31MWh	132.56MWh

## IV. CONCLUSION

This work focuses on the integration of flexible demand in the CoSES under the short-term market. Considering social welfare and network constraints, a bi-level optimization dispatch model for the optimal strategy of a gas, electricity and heat integrated energy system with smart buildings is proposed. In the proposed model, the smart buildings can realize the conversion between different energy carriers, in which customers have multiple options to satisfy their energy demand. Numerical studies substantiate that the proposed strategy cannot only optimize operation but also for setting transaction prices in markets. Meanwhile, we find that the build-in flexibility of smart buildings on the demand-side provides desirable flexible resources for the combined energy systems. This is specifically reflected in the improvement of total social welfare and wind accommodation.

## ACKNOWLEDGMENT

The first author is very grateful to China Scholarship Council for providing the scholarship.

## REFERENCES

- [1] K. Hansen, C. Breyer, and H. Lund, "Status and perspectives on 100% renewable energy systems," *Energy*, vol. 175, pp. 471–480, May. 2019.
- [2] Y. Zhang, P. E. Campana, Y. Yang, B. Stridh, A. Lundblad and J. Yan, "Energy flexibility from the consumer: Integrating local electricity and heat supplies in a building," *Applied Energy*, vol. 223, pp. 430–442, May. 2018.
- [3] C. Linvill, J. Lazar, D. Littell, J. Shipley and D. Farnsworth, "Flexibility for the 21<sup>st</sup> century power system," National Renewable Energy Laboratory (EREL), USA, NREL/TP-6A20-61721, Oct. 2019.
- [4] V. Kleinschmidt, T. Hamacher, V. Perić and M. R. Hesamzadeh, "Unlocking flexibility in multi-energy systems: A literature review," 17th International Conference on the European Energy Market (EEM), Stockholm, Sweden, Sept. 2020
- [5] V. Perić, T. Hamacher, A. Mohapatra et al., "CoSES laboratory for combined energy systems at TU Munich," IEEE Power & Energy Society General Meeting (PESGM), Montreal, QC, Canada, Aug. 2020.
- [6] F. Wang, L. Zhou, H. Ren et. al, "Multi-objective optimization model of source-load-storage synergetic dispatch for a building energy management system based on TOU price demand response," *IEEE Trans. Ind. Appl.*, vol. 52, no. 2, pp. 1017–1027, Dec. 2018.
- [7] C. Shao, Y. Ding, J. Wang and Y. Song, "Modeling and integration of flexible demand in heat and electricity integrated energy system," *IEEE Trans. Sustain. Energy*, vol. 9, no. 1, pp. 361–370, Jan. 2018.
- [8] G. C. Okwuibe, M. Wadhwa, T. Brenner, P. Tzscheutschler and T. Hamacher, "Intelligent bidding strategies in local electricity markets: a simulation-based analysis," IEEE Electric Power and Energy Conference (EPEC), Edmonton, Canada, Nov. 2020.
- [9] Z. Yi, Y. Xu, J. Zhou, W. Wu and H. Sun, "Bi-level programming for optimal operation of an active distribution network with multiple virtual power plants," *IEEE Trans. Sustain. Energy*, vol. 11, no. 4, pp. 2855–2867, Oct. 2020.
- [10] J. Zheng, Z. Zhou, J. Zhao and J. Wang, "Function method for dynamic temperature simulation of district heating network," *Applied Thermal Engineering*, vol. 123, pp. 682–688, May. 2017.
- [11] J. Fang, Q. Zeng, Z. Chen and J. Wen, "Dynamic optimal energy flow in the integrated natural gas and electrical power systems," *IEEE Trans. Sustain. Energy*, vol. 9, no. 1, pp. 188–197, Jan. 2018.
- [12] C. Ruiz and A. J. Conejo, "Pool strategy of a producer with endogenous formation of locational marginal prices," *IEEE Trans. Power Syst.*, vol. 24, no. 4, pp. 1855–1866, Nov. 2009.
- [13] Energinet.dk, "Energy data service" [Online]. Available: <https://www.energidataservice.dk/collections/production-and-consumption>.